Melting, Nonisothermal Crystallization Behavior and Morphology of Polypropylene/Random Ethylene–Propylene Copolymer Blends

Dong Wang,[1] Jungang Gao[2]

[1]*Advanced Materials Laboratory, Institute of Polymer Science & Engineering, Department of Chemical Engineering, Tsinghua University, Beijing, 100084, China*
[2]*College of Chemistry and Environmental Science, Hebei University, Baoding 071002, China*

Received 24 August 2003; accepted 23 March 2005
DOI 10.1002/app.22507
Published online in Wiley InterScience (www.interscience.wiley.com).

ABSTRACT: The melting, nonisothermal crystallization behavior and morphology of blends of polypropylene (PP) with random ethylene–propylene copolymer (PP-R) were studied by differential scanning calorimetry, polarized optical microscopy, scanning electron microscopy, and X-ray diffraction. The results showed that PP and PP-R were very miscible and cocrystallizable. Modified Avrami analysis was used to analyze the nonisothermal crystallization kinetics of the blends. The values of the Avrami exponent indicated that the crystallization nucleation of the blends was heterogeneous, the growth of the spherulites was tridimensional, and the crystallization mechanism of PP was not affected by PP-R. The crystallization activation energy was estimated using the Kissinger method. An interesting result was obtained with the modified Avrami analysis and the Kissinger method, whose conclusions were in good agreement. The addition of a minor PP-R phase favored an increase in the overall crystallization rate of PP. Maximum enhancing effect wass found to occur with a PP-R content of 20 wt %. The relationship between the composition and the morphology of the blends is discussed. J Appl Polym Sci 99: 670–678, 2006

Key words: polypropylene (PP); blends; crystallization; morphology

INTRODUCTION

Polypropylene (PP) is one of the most widely used polyolefin polymers, but its application in some fields is limited because of low fracture toughness at low temperature and high notch sensitivity at room temperature. Compounding PP with a dispersed elastomeric phase [e.g., ethylene–propylene–diene rubber (EPDM)] is widely practiced[1–5] because the rubber can increase the overall toughness of the PP matrix.[6] But the addition of elastomers often has negative effects on some properties of PP, such as stiffness and hardness.[7]

PP-R produced by copolymerization of propylene and ethylene is a new product of modified polypropylene that has received a great deal of attention in scientific studies[8–10] and is extremely attractive to the plastics industry.[11] During copolymerization with propylene, ethylene occasionally is embedded into the long propylene sequences. The embedded ethylene units disrupt crystallization of the propylene sequences, thus decreasing total crystallinity, after which decreases in the rigidity and melting point of PP occur. The copolymer is mainly composed of long propylene sequences with an occasional ethylene unit, such as propylene-propylene-ethylene, ethylene–propylene–ethylene, and propylene–ethylene–propylene. PP-R has been shown to have excellent thermal stability, aging resistance, and mechanical properties.[11] Further, PP-R is granular in form, and when blending with PP, it uses a convenient processing technology such as extrusion or injection molding, etc. Unlike with conventional EPDM, PP-R at 30 wt % of the content can more than double the impact strength of PP while maintaining basically the same PP tensile strength.[12]

It is well known that the physical properties of semicrystalline polymeric materials strongly depend on their crystallization and microstructure; thus, investigations of the crystallization behavior and morphology of polymer blends are important both theoretically and practically. In particular, the crystallization behavior during nonisothermal crystallization from melt is of increasing technological importance because these are those closest to actual industrial

Correspondence to: J. Gao (wdhbu@yahoo.com.cn).
Contract grant sponsor: Natural Science Foundation of Hebei Province, China; contract grant number: 201068.
Contract grant sponsor: Educational Science Foundation of Hebei Province, China; contract grant number: 2000105.

conditions. However, until now, such a detailed investigation of the PP/PP-R system has not been reported.

In this study the nonisothermal crystallization behavior of PP/PP-R blends were investigated in order to examine: (1) the phase behavior and possibility of cocrystallization of PP/PP-R blends, (2) the validity of the modified Avrami analysis for the nonisothermal crystallization of PP in the PP-R blends, and (3) the effect of PP-R on the PP crystallization mechanism. The morphology of the blends also was studied in order to investigate the effect of PP-R on blend microstructure.

EXPERIMENTAL

Materials and sample preparations

The PP [type T30S, d = 0.901 g/cm^3, melting flow index (230°C/2.16 kg) = 3.88 g/10 min, tacticity = 96.6%] used in this study was a commercial polymer supplied by Daqing Petrochemical Co. (Daqing, China). The PP-R sample [type RA130E, d = 0.905 g/cm^3, melting flowing index (230°C/2.16 kg) = 0.25 g/10 min] was obtained from Borealis. The concentration of ethylene was 3 wt %.

Blend samples were prepared by melt-blending on a two-roll mill at 180°C for 10 min. The weight-to-weight ratios (w/w) of PP/PP-R were 100 : 0, 90 : 10, 80 : 20, 70 : 30, 60 : 40, 40 : 60, 20 : 80, and 0 : 100. The melt of the blends was compressed in a electric-heat press for 5 min at 16 MPa and 180°C and cold-pressed for 10 min at 5 MPa in order to produce a 4-mm-thick sheet.

Thermal analysis

A Perkin-Elmer DSC-7 apparatus was used to investigate the melting and nonisothermal crystallization behavior of the blends. All the operations were carried out in a nitrogen environment. The temperature and melting enthalpy were calibrated with standard indium. Each sample weighed about 7.4 mg.

For melting behavior, samples were heated from room temperature to 210°C at a rate of 10°C/min. To erase the influence of thermal history, a second run was carried out after the melted samples were cooled to 50°C. As for nonisothermal crystallization, samples were heated from room temperature to 210°C, maintained at this temperature for 5 min, and then cooled to 50°C at various cooling rates: 2.5°C/min, 5°C/min, 10°C/min, and 20°C/min.

Morphology analysis

Polarized optical microscope (POM) micrographs were obtained with an XPT-7 polarized optical microscope equipped with an Olympus camera. Compression-molded film was sandwiched between a microscope slide and a cover glass. The samples were heated from room temperature to 210°C, maintained at this temperature for 5 min to allow complete melting, and then cooled to 140°C for isothermal crystallization for 1 h.

Scanning electron microscope (SEM) micrographs were taken on a KYKY model 1000B microscope according to the method of Campbell.[13] All microtomed surfaces of the blends were polished by polishing cream and then were chemically etched at room temperature for 1 h in a potassium permanganate solution according to the procedure suggested by Coccorullo.[14] The surfaces were rinsed with distilled water and dried for 5 h at 60°C in vacuum.

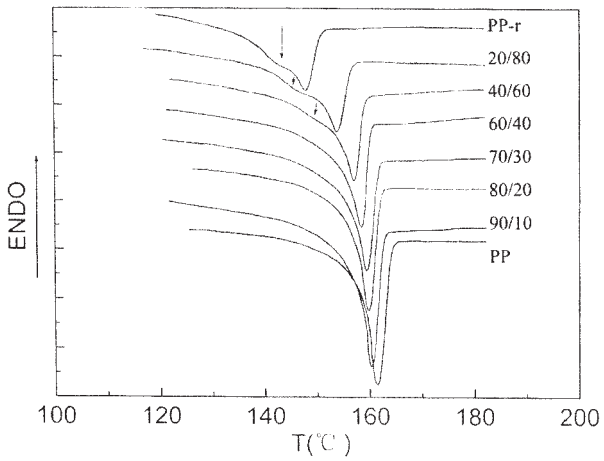

Figure 1 DSC melting curves of PP/PP-R blends. The heating rate was 10°C/min.

RESULTS AND DISCUSSION

Melting and crystallization behavior of PP/PP-R blends

Figure 1 shows the differential scanning calorimetry (DSC) melting curves of pure polymers and their blends. As can be seen from Figure 1, pure PP-R has a low melting temperature and at about 140°C shows a shoulder peak on the lower temperature side. It was shown that the copolymerization of ethylene with propylene for the PP-R was not homogeneous—the higher the ethylene content, the lower the melting temperature. The others had a high melting temperature. When PP-R content was less than 40%, the blends displayed only one melting peak, which is an indication of polymer miscibility. The apparent melting temperature (T_m) of the blends decreased with increasing PP-R content, from 161.2°C with pure PP to 147.5°C with pure PP-R (Table I), and the T_m of the PP/PP-R blends was between the T_m of pure PP and the T_m of PP-R, indicating that cocrystallization was character-

TABLE I
Melting Temperature (T_m) and Fusion Heat (ΔH_m) of PP/PP-R Blends

Sample	PP	90 : 10	80 : 20	70 : 30	60 : 40	40 : 60	20 : 80	PP-R
T_m (°C)	161.7	161.2	160.6	160.0	159.0	157.3	153.9	147.5
ΔH_m (J/g)	99.9	94.3	88.6	85.9	81.8	78.3	70.1	65.9
X_x (%)	43.94		39.67		37.26	35.12	33.09	32.04

X_x is crystallinity examined by X-ray diffraction.

istic of the blends. In addition, the fusion curves became broader with increasing PP-R content, meaning that their crystallinity and morphology changed. The small defective crystals that initially formed during nonisothermal crystallization because of the addition of PP-R were the metastable crystalline phase, which had a low melting temperature. After melting, the polymer chains trapped in such a phase could gain the proper mobility to form a more perfect crystalline phase. This was able to happen because the melting occurred at temperatures low enough for the supercooling to be large[15] but high enough for the chains to gain the proper mobility to form stable crystals. Thus, the wider peak was a result of the melting and recrystallization or reorganization of these defective crystals. Meanwhile, it also indicated that with increasing PP-R content, the spherulite became smaller and the number of defective crystals increased. This behavior was demonstrated further by POM analysis.

The heat of fusion (ΔH_m) of the PP/PP-R blends decreased regularly with PP-R content (see Table I). It also was shown that the PP-R component could decrease the total crystallinity of the blends. Feng et al.[9] reported that fusion heat decreased linearly with an increase in the ethylene component of PP-R. In the PP/PP-R blends, PP and PP-R are very miscible; thus, the main factor explaining the decreased ΔH_m of the PP/PP-R blends was the ethylene comonomer, which decreased the crystallinity of the blends.

Because the cocrystallization behavior of the two crystallizable polymers was strongly dependent on the crystallization speed (i.e., cooling rate from the melt),[16–18] the effect of cooling rate on the crystallization behavior of the PP/PP-R blends was investigated. Figure 2 shows the heating DSC thermograms for the PP/PP-R (70 : 30) blends prepared at various cooling rates. As shown in Figure 2, only one fusion peak was observed regardless of the cooling rate. Cho et al.[19] reported that at lower cooling rates (1°C/min, 5°C/min, 10°C/min), two melting peaks (phase separations) could occur, whereas at higher cooling rates (30°C/min, 40°C/min), a single melting peak (cocrystallization) would occur in the PP/maleated PP blends. However, all PP/PP-R (70 : 30) blends showed a single melting peak, regardless of cooling rate. Therefore, it can be concluded that PP/PP-R forms cocrystal. The T_m of the 70 : 30 blends slightly decreased as the cooling rate increased, because with the increased cooling rate, crystallization occurred at a lower temperature and had more defects.

As an example, Figure 3 shows the typical crystallization exotherms of PP/PP-R (80 : 20) blends at various cooling rates. All the crystallization exotherms were found to reflect the cocrystallization of PP/PP-R melt. Peak temperature (T_p) and heat of crystallization

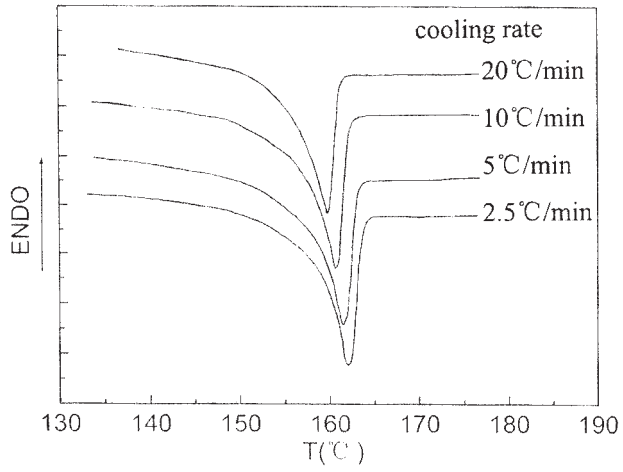

Figure 2 DSC melting curves of PP/PP-R (70:30) blends prepared at various cooling rates. The heating rate was 10°C/min.

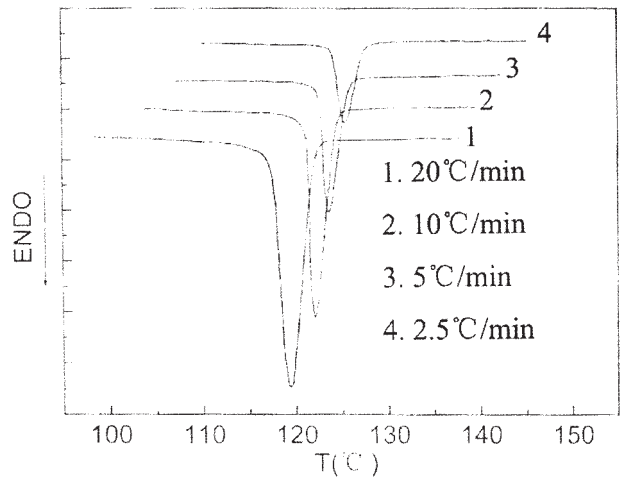

Figure 3 DSC nonisothermal crystallization curves of PP-R (80:20) blends at various cooling rates.

TABLE II
Nonisothermal Crystallization Parameters of PP/PP-R Blends at Different Cooling Rates

Sample	D (°C/min)	n	k'	? (min)	T_p (°C)	ΔH_c (J/g)	E_a (kJ/mol)
PP	2.5	2.72	0.18	3.75	121.0	96.5	437.90
	5.0	2.66	0.54	1.85	120.0	93.5	
	10	2.58	0.85	1.08	117.6	93.7	
	20	2.60	0.98	0.61	115.2	90.7	
20% PP-R	2.5	2.70	0.26	3.09	125.8	87.1	398.47
	5.0	2.68	0.70	1.71	124.4	85.5	
	10	2.52	0.97	1.01	122.4	81.8	
	20	2.87	1.09	0.50	119.1	79.0	
40% PP-R	2.5	2.80	0.23	3.14	124.8	81.0	408.45
	5.0	2.74	0.64	1.73	123.9	74.9	
	10	2.63	0.90	0.91	121.0	73.2	
	20	2.55	1.04	0.54	118.6	68.2	

(ΔH_c), estimated as a function of cooling rate, are listed in Table II. As shown in Table II, with an increase in cooling rate, the T_p of the pure PP and the PP/PP-R blends shifted to a lower temperature. The decrease in T_p with a faster cooling rate was a result of the crystallization rate being slower than the experimental cooling rate.[20] At a slower cooling rate, PP had enough time to crystallize and the spherulite had little defects and therefore a higher T_p. However, for a given cooling rate (10°C/min), the T_p shifted to a higher temperature with increasing PP-R content of the blend. The T_p increased from 117.6°C in pure PP to 122.4°C in the blend containing 20% PP-R and then decreased to 110°C in pure PP-R (see Fig. 4). The highest increase of T_p, about 4.8°C, was obtained for the PP/PP-R (80 : 20) blends. Similar crystallization behavior was reported for PP/PB-1 blends by Shieh et al.[21] A possible interpretation of the results in the PP/PP-R blends, in which the PP-R had a higher molecular weight and viscosity [*MFI* (230°C/2.16 kg) = 0.25 g/10 min], the PP molecular chains aggregated to the long PP-R molecular chains and crystallized. However, with the PP-R content increased in certain blend compositions, the PP-R started to form a continuous phase, and the crystallization of the blend tended to bulk crystallization of PP-R; thus, the crystallization of PP was retarded, and then the T_p decreased again. From this, it is clear that crystallization behavior was enhanced with a lower PP-R content and then decreased slightly as the PP-R content increased.

For all the samples, the heat of crystallization (ΔH_c) decreased with blend composition, indicating that the total crystallinity of the blends decreased with the addition of PP-R, in agreement with the ΔH_m values obtained in the DSC heating runs.

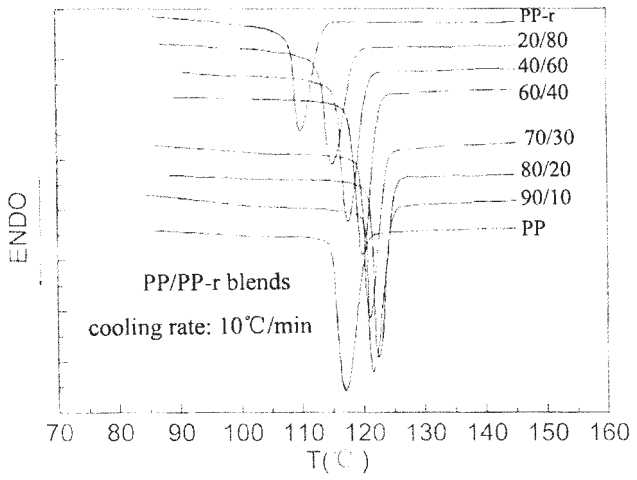

Figure 4 DSC nonisothermal crystallization curves of PP/PP-R blends. The cooling rate was 10°/min.

Nonisothermal crystallization kinetics

To date, several analytical methods have been developed to describe the nonisothermal crystallization kinetic of polymers: (1) modified Avrami analysis,[22–24] (2) Ozawa analysis,[25–26] (3) Ziabicki analysis,[27–28] and (4) other types of analyses[29–32] such as Mo Z.S.[29] analysis. In the present study, modified Avrami analysis was used to describe the nonisothermal crystallization kinetics of PP/PP-R blends.

Modified Avrami analysis

The Avrami equation[24,33–34] has been widely used to describe isothermal crystallization kinetics of polymers:

$$1 - X_t = \exp(-kt^n) \quad (1)$$

where X_t is the relative crystallinity, k is the growth rate constant, and n is the Avrami exponent. Here, the value of the Avrami exponent n depends on the nucleation mechanism and growth dimension, and pa-

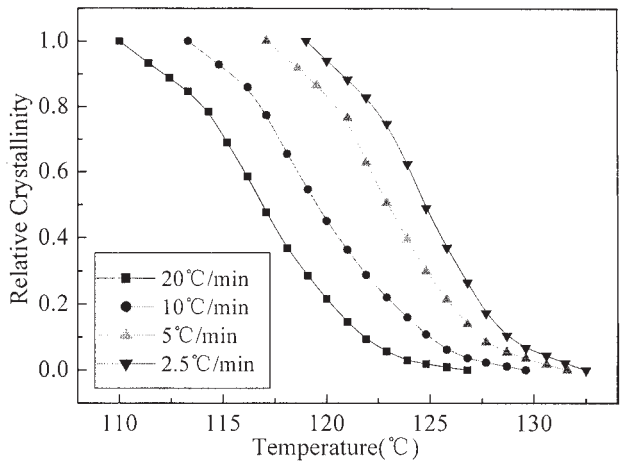

Figure 5 Plot of relative crystallinity, X_t, versus crystallization temperature, T, of PP/(20%) PP-R blends for nonisothermal crystallization at various cooling rates.

rameter k is a function of the nucleation and the growth rate. Relative crystallinity, X_t, as a function of crystallization time is defined as:

$$X_t = \frac{\int_0^x (dH_C/dT)dT}{\int_0^{\infty} (dH_C/dT)dT} \quad (2)$$

where dHc/dT is the rate of heat evolution, and t_0 and t_∞ are the times at which crystallization starts and ends, respectively.

The Avrami equation can be modified in order to describe nonisothermal crystallization.[22–23,35–36] For nonisothermal crystallization at a chosen cooling rate, relative crystallinity, X_t, is a function of crystallization temperature. That is, eq. (2) can be rewritten as follows:

$$X_t = \frac{\int_{T_0}^{T} (dH_C/dT)dT}{\int_{T_0}^{T_\infty} (dH_C/dT)dT} \quad (3)$$

where T is the crystallization temperature, T_0 and T_∞ represent the onset and end crystallization temperatures, respectively.

As an example, Figure 5 shows the relative crystallinity of PP/(20%) PP-R blends at various cooling rates. All curves in Figure 5 show a reversed sigmoidal shape, indicating a fast primary process during the initial stages and a slower secondary process during the later stages. The plot of X_t versus T shifts to the low-temperature region as the cooling rate increases, indicating that crystallization was enhanced as the temperature decreased. That is because the nucleation and growth parameters were strongly dependent on temperature.[37] After passing the maximum in the heat flow curves, a large fraction of crystallinity developed by slower, secondary kinetic processes. The slower cooling rate provided more fluidity and diffusivity for the molecules because of the relatively lower viscosity and more time for perfection crystallization, thus inducing much higher crystallinity at higher temperature than for the samples cooled with fast cooling rates, as shown in Figure 5.

Crystallization temperature can be converted to crystallization time, t, using the equation[28,35]

$$t = \frac{T_0 - T}{D} \quad (4)$$

where D is the cooling rate. Using eq. (4), the temperature axis in Figure 5 can be transformed into time scale, as shown in Figure 6. The sigmoidal shape of the curves suggests that the extended Avrami analysis is applicable for nonisothermal crystallization of PP/PP-R blends. Meanwhile, the crystallization half time, $t_{1/2}$, can be calculated directly from the relative crystallinity versus time plot,[24,38] as shown in Table II.

If eq. (1) is rewritten in a double logarithm form as

$$\ln[-\ln(1 - X_t)] = \ln(k) + n \ln(t) \quad (5)$$

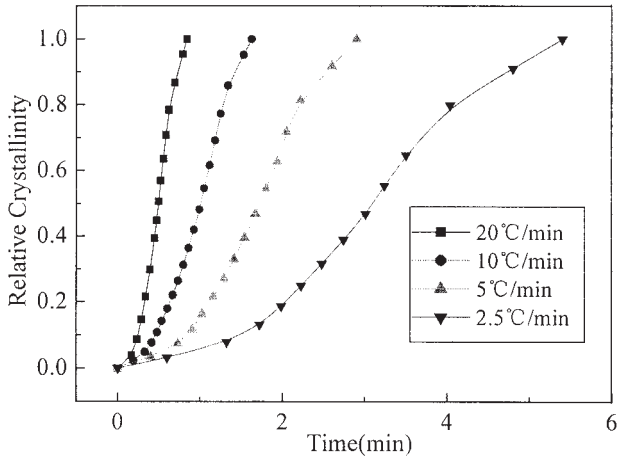

Figure 6 Plot of relative crystallinity, X_t, versus crystallization time, t, of PP/(20%) PP-R blends for nonisothermal crystallization at various cooling rates.

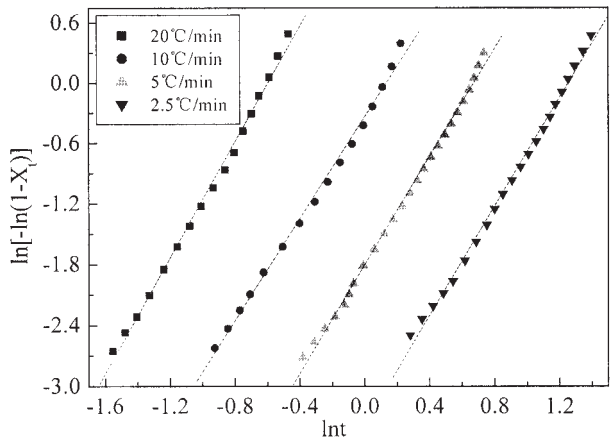

Figure 7 Avrami plot of PP/(20%) PP-R blends for nonisothermal crystallization at various cooling rates.

then the Avrami parameters can be estimated from the $\ln[-\ln(1 - X_t)]$ versus $\ln t$. Here, the crystallization rate of nonisothermal crystallization depends on the cooling rate. Thus, the crystallization rate constant, k, should be corrected adequately. Assuming a constant cooling rate, the crystallization rate constant can be corrected as[35] $\ln k' = \ln k/D$.

Figure 7 shows the plot of $\ln[-\ln(1 - X_t)]$ versus $\ln t$ for nonisothermal crystallization of PP/(20%) PP-R blends. All lines in Figure 7 are parallel to each other, shifting to less time with increasing cooling rate. This implies that the nucleation mechanism and crystal growth geometries were similar, although the cooling rates were different. The values of the Avrami parameters, estimated from the plot of $\ln[-\ln(1 - X_t)]$ versus $\ln t$, are listed in Table II. Regardless of the cooling rate, the Avrami exponent, n, for the pure PP was in the range of 2.58–2.72, which is in good agreement with reports in the literature for measurements performed under nonisothermal[39] and isothermal[37] conditions, indicating heterogeneous nucleation and tridimensional growth of spherulites. The Avrami exponents for the PP/PP-R blends were in the range of 2.52–2.87, regardless of the blend composition and cooling rate, showing that the crystallization mechanism of PP was not affected in the presence of PP-R.

However, the crystallization rate was dependent on the blend composition and cooling rates. On the one hand, for the pure PP, the crystallization rate constant (k') increased with cooling rate, whereas the crystallization half time ($t_{1/2}$) decreased with increasing cooling rate (see Table II). Similar trends in both the k' and $t_{1/2}$ were observed for the PP/(20%) PP-R and PP/(40%) PP-R blends. On the other hand, both the k' and $t_{1/2}$ also were influenced by the addition of PP-R—that is, at the same cooling rate, the k' increased to the maximal crystallization rate (20% PP-R content) and then slightly decreased with an increase in PP-R content, with the $t_{1/2}$ adversely affected. It was conclusively shown that the crystallization rate was accelerated by increasing the cooling rate or was enhanced with the introduction of a small quantity of PP-R in PP, results that corresponded to the crystallization behavior analysis.

Activation energy of nonisothermal crystallization

For nonisothermal crystallization, the crystallization activation energy (E_a) can be estimated from the variation of crystallization peak temperature (T_p) with cooling rate, D, by the Kissinger approach:[40]

$$\frac{d[\ln(D/T_p^2)]}{d(1/T_p)} = -\frac{E_a}{R} \tag{6}$$

where R is the universal gas constant.

The Kissinger plot is the plot of $\ln(D/T_p^2)$ versus $1/T_p$ for PP/PP-R blends, as shown in Figure 8. The E_a was estimated to be 437.90 kJ/mol for pure PP, 398.47 kJ/mol for the PP/(20%) PP-R blends and 408.45 kJ/mol for the PP/(40%) PP-R blends (see Table II). In comparison, the E_a of the pure PP was higher than that of the PP/PP-R blends, and the E_a of the PP/(40%) PP-R blends was higher than that of the PP/(20%) PP-R blends. From a kinetic viewpoint, the activation energy could be correlated to the crystallization rate. As described earlier in this study, there was a relative decrease in the crystallization rate in the order of PP/(20%) PP-R blends > PP/(40%) PP-R blends > pure PP (see Table II). That is, the lower activation energy of crystallization drove the more rapid crystallization rate, a result consistent with the previous conclusion.

Morphology analysis

Figure 9 shows the POM micrographs of PP/PP-R blends that have been isothermal crystallized at 140°

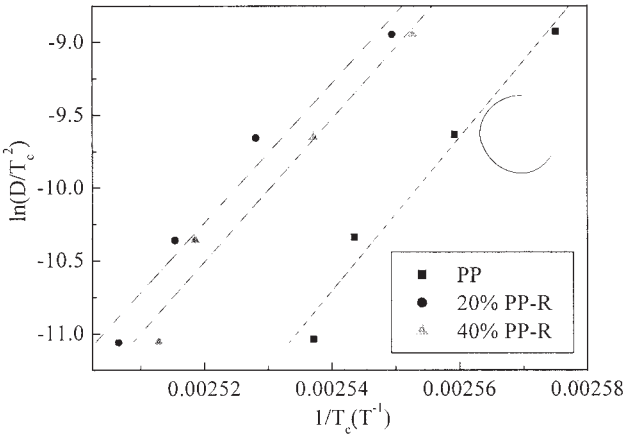

Figure 8 Kissinger plot of $\ln(D/T_p^2)$ versus $1/T_p$ of PP/PP-R blends for nonisothermal crystallization at different PP-R contents.

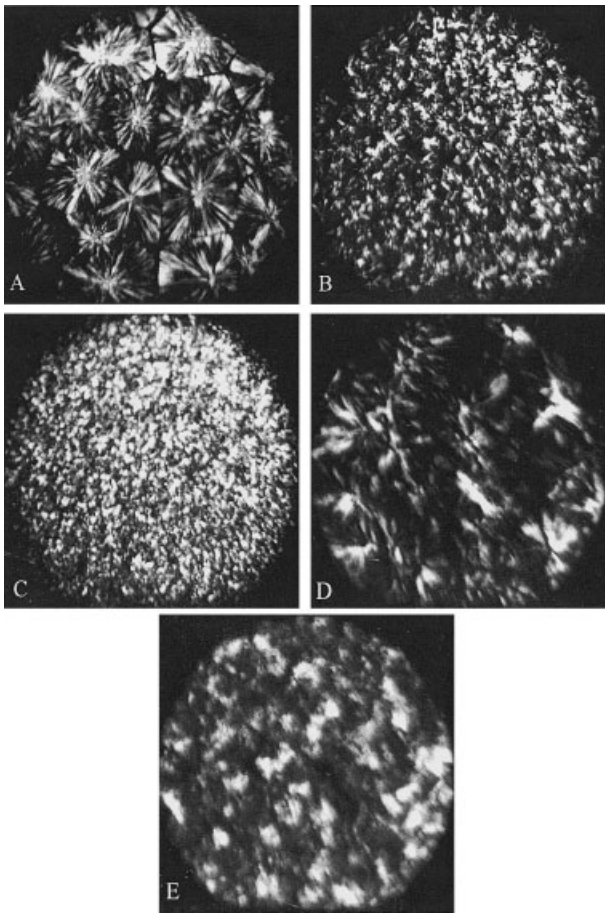

Figure 9 POM micrographs of PP/PP-R blends: (A) pure PP (100×), (B) 10% PP-R (100×), (C) 20% PP-R (100×), (D) 10% PP-R (400×), (E) 20% PP-R (400×).

for 1 h. As shown in Figure 9(a), the pure PP revealed well-defined and large spherulitic morphology. The spherulites grew, impinged on each other, and formed particular polygonal spherulites with clear boundaries. With the addition of 10% PP-R, spherulite size promptly decreased, and with less perfection, the right-angled intersection disappeared, the sharp spherulite boundaries became more diffuse, and interspherulitic interaction increased [Fig. 9(b)]. At a higher PP-R content [Fig. 9(c)], the spherulites could not be clearly observed. Figure 9(d,e) shows the magnified POM micrographs of PP/(10%) PP-R and PP/(20) PP-R blends, indicating that less perfect spherulites still formed, although they were distorted and very small. Overall, the addition of PP-R greatly affected the spherulite size and morphology of PP. Spherulite size immediately decreased with increasing PP-R content. This resulted from the cocrystallization and crystallizability of PP being disrupted by the higher concentration of PP-R. The PP molecular chains were more difficult to pack in an ordered manner than those of pure PP; this caused a large number of spherulites to grow in a limited space. Therefore, perfect spherulites cannot form at a higher concentration of PP-R. In addition, the large number of nucleus centers caused additional crystalline defects and led to low crystallinity.

Further demonstrating the results of POM are the SEM micrographs of the etched surfaces in the potassium permanganate solution, shown in Figure 10. The pure PP had a coarse surface [Fig. 10(a)], whereas the PP/(30%) PP-R blend had a relatively smooth appearance [Fig. 10(b)]. With an increase in the PP-R content, the PP/(60%) PP-R and pure PP-R again showed a coarser surface [Fig. 10(c,d)] than that of the PP/(30%) PP-R blend. This means the addition of PP-R into PP had a great effect on blend microstructure. Pure PP had the largest-sized spherulites [as shown in Fig. 9(a)], a large defect between spherulites, and a loose structure formed by large and perfect spherulites. It was easy to oxidize the noncrystallization regions in the potassium permanganate solution. With the addition of PP-R, spherulite size and perfection greatly decreased, and the compactness of the blend structure increased. For this structure, oxidative etching of the noncrystallization region became difficult; therefore, the PP/(30%) PP-R blend showed a relatively smooth surface. In conclusion, these results were in good agreement with the POM analysis.

Figure 11 shows X-ray diffraction (XRD) patterns for PP, PP-R, and their blends. The strong diffraction peaks were at the diffraction angles 2θ of 14.00°, 16.79°, 18.48°, and 21.80° (a doublet), of which the former three peaks corresponded to (110), (040), and

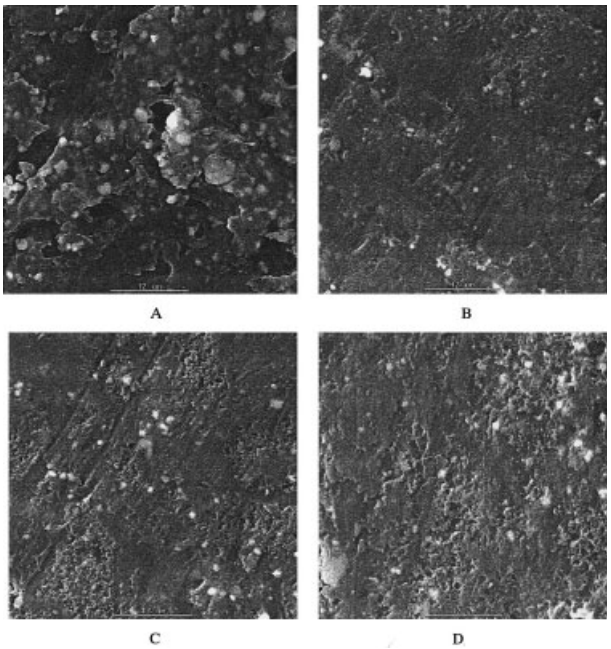

Figure 10 SEM micrographs of the etched surface in the potassium permanganate solution: (A) pure PP, (B) 30% PP-R, (C) 60% PP-R, (D) pure PP-R.

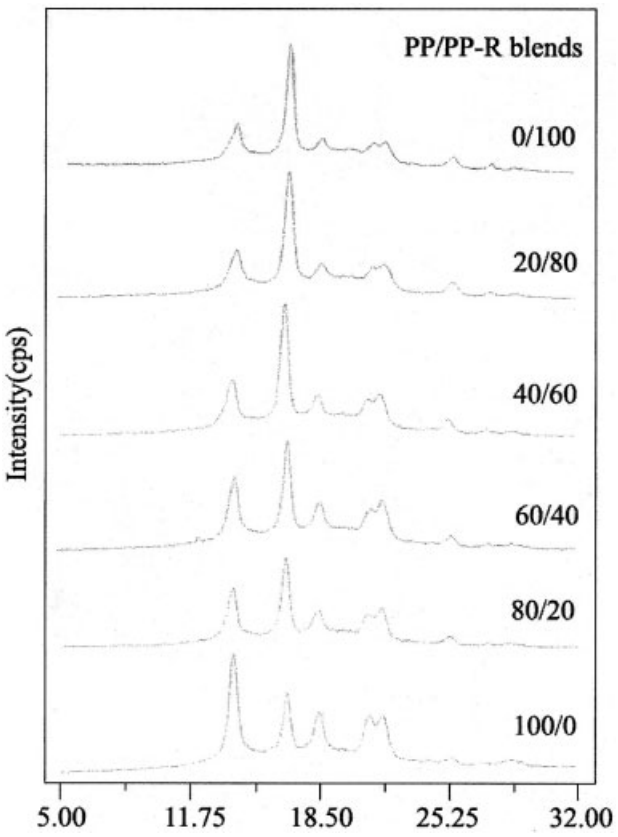

Figure 11 XRD patterns of PP/PP-R blends.

(130) planes, respectively, and were characteristic of the typical α-form monoclinic structure of PP.[41–42] Figure 11 demonstrates that the PP, PP-R, and their blends prepared from the melt all showed only the α crystal form. For the blends, the intensity of the PP peak decreased with an increase in PP-R content. The broadened background scattering area of the curves suggested the presence of an amorphous structure. The crystallinity could be estimated with the following formula[43]:

$$\text{Crystallinity (\%)} = \frac{S_c}{S_c + S_a} \times 100 \qquad (7)$$

where S_c is the area of crystallization and S_a is the background area. As shown in Table I, the crystallinity, X_x, linearly decreased with the blend composition, in good agreement with the nonisothermal crystallization process and DSC heating runs.

CONCLUSIONS

(1) The single peak during the melting and crystallization process indicated that PP and PP-R were very miscible and that there was cocrystallization. The crystallinity of the blends decreased with an increasing PP-R content.
(2) Investigation of the nonisothermal crystallization kinetics of the blend was accomplished fairly well by modified Avrami analysis. The values of the Avrami exponent were 2.52–2.87, regardless of the cooling rate and blend composition, indicating that the crystallization nucleation was heterogeneous, the growth of spherulites was tridimensional, and the nucleation and growth mechanism of the PP was not affected by the addition of PP-R.
(3) The crystallization rate of the blends was influenced by the composition as well as the cooling rate. At the same cooling rate, the crystallization rate increased with increasing PP-R content to 20% and then decreased slightly.
(4) The POM results showed that spherulite morphology and size were greatly affected by the PP-R, and the addition of PP-R resulted in a prompt decrease in spherulite size and an increase in the structural compactness of the blends. Both the SEM and the XRD results showed that the crystallinity of the blends decreased with increasing PP-R content and that only an α-form monoclinic structure was formed.

References

1. Karger-Kocsis, J.; Kalló, A.; Kuleznev, V. N. Polymer 1984, 25, 279.
2. Coppola, F.; Greco, R.; Martuscelli, E.; Kammer, H. W. Polymer 1987, 28, 47.
3. Tam, W. Y.; Cheung, T.; Li, R. K. Y. Polym Test 1996, 15, 452.
4. Van der Wal, A.; Mulder, J. J.; Oderkerk, J.; Gaymans, R. J. Polymer 1998, 39, 6781.
5. Yokoma, Y.; Ricco, T. J Appl Polym Sci 1997, 66, 1007.
6. Karger-Kocsis, J. Polypropylene—Structure, Blends and Composites; Chapman & Hall: London, 1994.
7. Qiu, G. X.; Raue, F.; Ehrenstein, G. W. J Appl Polym Sci 2002, 83, 3029.
8. Hayashi, T.; Inoue, Y.; Chujo, R. Macromolecules 1988, 21, 3139.
9. Feng, Y.; Hay, J. N. Polymer 1998, 39, 6589.
10. Saga, K.; Shiono, T.; Doi, Y. Macromolecules Chemisty 1988, 189, 1531.
11. Zhao, M.; Gao, J. G.; Deng, K. L.; Zhao, X. Y. New Materials of Modified Polypropylene; Chemical Industry Press: Beijing, 2002.
12. Wang, D.; Gao, J. G.; Li, S. R.; Wang, H. China Plastics 2003, 17, 19.
13. Campbell, D.; White, J. R. Polymer Characterization; Chapman and Hall: New York, 1989.
14. Coccorullo, I.; Pantani, R.; Titomanlio, G. Polymer 2003, 44, 307.
15. Papageorgiou, G. Z.; Karayannidis, G. P. Polymer 2001, 42, 2637.
16. Sham, C. K.; Guerra, G.; Karasz, F. E.; Macknight, W. J. Polymer 1988, 29, 1016.
17. Lee, J. C.; Namura, S.; Kondo, S.; Abe, A. Polymer 2001, 42, 5453.
18. Runt, J.; Jin, L.; Talibuddin, S.; Davis, C. R. Macromolecules 1995, 28, 2781.

19. Cho, K. W.; Li, F. K.; Choi, J. S. Polymer 1999, 40, 1719.
20. Park, J. Y.; Kwon, M. H.; Park, O. O. J Polym Sci: Polym Phys 2000, 38, 3001.
21. Shieh, Y. T.; Lee, M. S.; Chen, S. A. Polymer 2001, 42, 4439.
22. Herrero, C. H.; Acosta, J. L. Polymer 1994, 26, 786.
23. De Juana, R.; Jauregui, A.; Calahora, E.; Cortazar, M. Polymer 1996, 37, 3339.
24. Lee, S. W.; Ree, M.; Park, C. E.; Jung, Y. K.; Park, C. S.; Jin, Y. S.; Bae, D. C. Polymer 1999, 40, 7137.
25. Ozawa, T. Polymer 1971, 12, 150.
26. Ozawa, T. Polymer 1978, 19, 1142.
27. Ziabicki, A. Coll Polym Sci 1974, 6, 252.
28. Ziabicki, A. Appl Polym Symp 1967, 6, 1.
29. Liu, T. X.; Mo, Z. S.; Wang, S. E.; Zhang H. F. Polym Eng Sci 1997, 37, 568.
30. Caze, C.; Devaux, E.; Crespy, A.; Cavrot, J. P. Polymer 1997, 38, 497.
31. Nakamura, K.; Katayama, K.; Amano, T. J Appl Polym Sci 1973, 17, 1031.
32. Chan, T. W.; Isayev, A. I. Polym Eng Sci 1994, 34, 461.
33. Avrami, M. J Chem Phys 1939, 7, 1103.
34. Avrami, M. J Chem Phys 1940, 8, 212.
35. Jeziorny, A. Polymer 1978, 19, 1142.
36. Tobin, M. C. J Polym Sci, Polym Phys 1974, 12, 399.
37. Seo, Y. S.; Kim, J. H.; Kin, K. U.; Kim, Y. C. Polymer 2000, 41, 2639.
38. Xu, W.; Ge, M.; He, P. J Appl Polym Sci 2001, 82, 2281.
39. Yu, J.; He, J. Polymer 2000, 41, 891.
40. Kissinger, H. E. J Res Natl Bur Stds (US) 1956, 57, 217.
41. Jang, G. S.; Cho, W. J.; Ha, C. S. J Polym Sci: Polym Phys 2001, 39, 1001.
42. Lovinger, A. J.; Chua, J. O.; Gryte, C. C. J Polym Sci: Polym Phys Ed 1977, 15, 64.
43. Guan, Y.; Wang S. Z.; Zheng, A. N.; Xiao, H. N. J Appl Polym Sci 2003, 88, 872.